Projection of future changes in the frequency of intense tropical cyclones

Masato Sugi[1], Hiroyuki Murakami[1, 2] and Kohei Yoshida[1]

1 Meteorological Research Institute, Tsukuba, Japan
2 Geophysical Fluid Dynamics Laboratory, Princeton, NJ, U.S.A

June 2, 2016
To be submitted to Climate Dynamics

Corresponding author address: Masato Sugi, Meteorological Research Institute, 1-1 Nagamine, Tsukuba, Ibaraki, Japan, E:mail: msugi@mri-jma.go.jp

Abstract

Recent modeling studies have consistently shown that the global frequency of tropical cyclones will decrease but that of very intense tropical cyclones may increase in the future warmer climate. It has been noted, however, that the uncertainty in the projected changes in the frequency of very intense tropical cyclones, particularly the changes in the regional frequency, is very large. Here we present a projection of the changes in the frequency of intense tropical cyclones estimated by a statistical downscaling of ensemble of many high-resolution global model experiments. The results indicate that the changes in the frequency of very intense (category 4 and 5) tropical cyclones are not uniform on the globe. The frequency will increase in most regions but decrease in the south western part of Northwest Pacific, the South Pacific, and eastern part of the South Indian Ocean.

1. Introduction

Knutson et al. (2010) concluded that existing modeling studies consistently project decreases in the globally averaged frequency of tropical cyclones, and higher resolution modeling studies typically project substantial increases in the frequency of the most intense cyclones. Recently the confidence of these conclusions is further enhanced by many additional high-resolution model experiments (IPCC 2013, Murakami et al. 2015; Roberts et al. 2015; Wehner et al. 2015; Walsh et al. 2016). However, it is noted that there remains a very large uncertainty in the projected changes in the very intense tropical cyclone frequency, particularly in the regional frequency (Figure 14.17 of IPCC 2013). The uncertainty is so large that it is difficult to draw any useful information for risk assessment. The main reason for the very large uncertainty is a lack of many high resolution global models that realistically simulate very intense (category 4 and 5) tropical cyclones.

To make a more reliable estimation of the changes in very intense tropical cyclone frequency, Knutson et al. (2013, 2015) employed a dynamical downscaling method. Knutson (2015) downscaled all the tropical storms simulated by the higher resolution global atmospheric model (GFDL HiRAM; 50km grid) by using the GFDL hurricane

model (nested grid model; 6km grid near the storm). Their results indicate that the frequency of very intense tropical cyclones will increase in most ocean basins but it will decrease in the South Pacific, the eastern Indian Ocean and southern section of the Northwest Pacific. The results of Knutson et al. (2015) seem to be considerably more reliable than IPCC (2013). However, their results are based on a single 20 year (tropical cyclone season) global model simulation, and the number of simulated very intense tropical cyclones is still insufficient to make a statistically reliable estimation of the change.

In the present study, we estimate the changes in intense tropical cyclone frequency based on a statistical downscaling of ensemble of many high-resolution global model experiments. In Section 2, the experiment data and the statistical downscale method are described. The main results are presented in Section 3, followed by discussions in Section4 and conclusions in Section 5.

2. Data and method

We used simulation data from an ensemble of many high resolution global model experiments conducted at Meteorological Research Institute (MRI) (Murakami et al. 2012a, 2012b; Sugi et al. 2012). These experiments are listed in Table 1. The experiments are 25 year simulations of the present day (PD) climate (11 members) and the future global warming (GW) climate (29 members). Models used for the experiments are various versions of MRI-AGCM3, with horizontal resolution 60km and 20km, and with three different convection schemes. The sea surface temperature (SST) for the PD experiments (1979-2003) is the observed SST (HadISST1; Rayner et al. 2003). For the GW experiments (2075-2099), seasonally varying average SST change estimated by the 18 member ensemble of Coupled Model Intercomparison Project phase 3 (CMIP3) models is added to the PD experiment SST (see Murakami et al. 2012a for the further detail). The atmospheric concentration of greenhouse gases and aerosols in the experiments is based on the Intergovernmental Panel on Climate Change (IPCC) A1B scenarios.

Among the 40 experiments listed in Table 1, the only two experiments (P11 and

F29) using the 20km grid AGCM3.2 could simulate very intense tropical cyclones realistically. In all the other experiments, the intensity of simulated tropical cyclones is generally much weaker than that of observed tropical cyclones and very intense tropical cyclones are not simulated. To estimate the possible future changes in the frequency of very intense tropical cyclones using these experiments, some downscaling method is needed for these experiments. Here we employ a statistical downscaling method, in which the intensity bias of the simulated tropical cyclones is corrected by a statistical method. The statistical method of bias correction is similar to the method used by Zhao and Held (2010). As shown in Fig.1, we use a cumulative distribution function (CDF). The wind speed of a simulated tropical cyclone is adjusted to the wind speed of the observed tropical cyclone with the same probability in the CDF. We applied the statistical bias correction for each 5 degree latitude band in each ocean basin. This is because the intensity biases are not the same everywhere. As the model tends to develop tropical cyclones slowly compared to the observation, the intensity of simulated tropical cyclones tends to be weaker in the low latitudes and stronger in the high latitudes. This bias has been noted as a northward bias of intense tropical cyclones in the northern hemisphere (Murakami et al. 2012a). By applying the bias correction to each latitude band, such a northward bias is also reduced. Figure 2 shows the observed, simulated and adjusted tropical cyclone tracks with intensity indicated by different colors. The intensity of simulated tropical cyclones in the experiment P10 using a 60km grid model (Fig.2b) is generally much weaker than that of observed tropical cyclones (Fig.2a), while the intensity of the adjusted tropical cyclones (Fig. 2c) is close to that of observed tropical cyclones.

As observation data of tropical cyclone climatology, we used dataset available on Unisys corporation website (2012) which consists of best-track TC data compiled by the National Hurricane Center (NHC) and Joint Typhoon Warning Center (JTWC).

3. Results

We examine the changes in tropical cyclone number (TC number) and tropical cyclone days (TC days) in various intensity categories: all tropical storms (cat 0-5;

126 Vmax≥17m/s), hurricanes (cat 1-5; Vmax≥33m/s), major hurricanes (cat 3-5;
127 Vmax≥50m/s) and very intense tropical cyclones (cat 4-5; Vmax≥59m/s). For the TC
128 number, the intensity category is defined by the lifetime maximum wind speed for each
129 tropical cyclone. For the TC days, the intensity category is defined by the maximum
130 wind speed of a tropical cyclone every 6 hours, and the duration (number of days) of the
131 tropical cyclone staying in each category is calculated.
132 Table 2 summarizes the statistics of TC numbers in various intensity categories for
133 global domain and by ocean basins. The model simulation data denoted by P and F are
134 the ensemble mean of 11 member PD experiments (P1-P11) and 29 member GW
135 experiments (F1-F29), respectively. These experiments are different from each other by
136 resolution (20km or 60km), SST anomaly for the GW experiments, convection schemes
137 (Arakawa-Shubert scheme (AS), Yoshimura scheme (YS) or Kain-Fritch scheme (KF))
138 and initial conditions. All the simulation data are adjusted by the intensity bias
139 correction as described in the previous section.
140 The average global tropical cyclone number simulated by PD experiments in each
141 category is comparable to observation, with a little overestimation for cat 1-5 and cat
142 3-5, and underestimation for cat 4-5. The global number of all tropical storms (cat 0-5)
143 significantly (21%) decreases in the future warmer climate, while the more intense
144 tropical cyclones show smaller decrease, with little (0.7%) decrease in very intense
145 tropical cyclones (cat 4-5). The number of all tropical storms (cat 0-5) in each ocean
146 basin significantly (10-28%) decreases, although the changes are not statistically
147 significant for North Indian Ocean and Northeast Pacific Ocean. The changes in number
148 of tropical cyclones in more intense categories by ocean basins are not generally
149 statistically significant, although the fractional changes in some ocean basins are large.
150 The global changes (F-P) in cat 1-5 and cat 3-5 are contributed by Northeast Pacific
151 Ocean. The small global change in the number of very intense tropical cyclones (cat
152 4-5) results from a mixture of increase and decrease in various ocean basins.
153 The similar statistics for TC days is shown in Table 3. The simulated global TC
154 days in cat 0-5 are underestimated, indicating that the average lifetime of simulated

tropical cyclones (4.4 days) is shorter than that of observation (4.9 days). The TC days of simulated tropical cyclone in more intense categories are generally comparable to observation, with somewhat overestimation in cat 3-5 and underestimation in cat 4-5. The TC days in cat 0-5 significantly (8-33%) decrease globally and in each ocean basins, although the changes in the North Indian Ocean and the Northeastern Pacific Ocean are not statistically significant. The TC days in cat 1-5 decrease globally and in most ocean basins, while they increase in the Indian Ocean. These changes are not statistically significant except for the South Pacific Ocean. The TC days in more intense categories (cat 3-5 and cat 4-5) increase globally and in most ocean basins except for the South Pacific Ocean. These changes, however, are also not statistically significant except for the South Pacific Ocean.

Figure 3 shows the geographical distributions of the occurrence frequency (TC days) of very intense tropical cyclones (cat 4-5) in the observation, the ensemble means of PD and GW experiments and their difference. The TC days shown in Fig.3 are TC days per decade in each 5˚ x 5˚ grid box. The geographical distribution of the TC days of the PD simulation (Fig.3b) agrees well with that of observation (Fig.3a), although we can see some differences in these distributions. We consider that the part of the differences is rather expected because the PD simulation is an ensemble mean of the 11 members, while the observation is a single realization. As shown in Fig. 3d, the TC days of very intense tropical cyclones increase in most regions in the Northern Hemisphere except for southwestern part of the Northwest Pacific, the Northeast Pacific and westernmost part of the North Atlantic. In the Southern Hemisphere, the TC days decrease in most part except for the western part of the South Indian Ocean. Because the TC days decrease in some part but increase in other part of the Northwest Pacific Ocean or the Northeast Pacific Ocean, the changes are relatively small when averaged over these ocean basins (see Table 2). It is interesting to note that the pattern of the changes in TC days shown in Fig. 3d is similar to that shown in Knutson et al. (2015).

The geographical distributions of the changes in TC days in various intensity categories are shown in Fig. 4. The pattern of changes in TC days in cat 3-5 is similar to

those of cat 4-5, but the areas of decreasing TC days expand a little. The patterns of changes in TC days in cat 1-5 and cat 0-5 is also similar to those of cat 4-5, but the areas of decreasing TC days further expand, and in cat 0-5 the areas of decreasing TC days dominate the entire globe except for the central North Pacific Ocean, south western part of the South Indian Ocean, northern part of Arabian Sea and northwestern part of the Bay of Bengal.

4. Discussion

(a) Statistical significance

In the previous section, we have noted that the TC numbers or TC days of all tropical storms (cat 0-5) decrease globally and by ocean basins and these changes are statistically significant. On the other hand, the changes are not statistically significant for the tropical cyclones in more intense categories (Table 2). Figure 5 shows the geographical distribution of statistically significant changes in TC days in each intensity category. In Fig.5, p-value is calculated for each 5˚ x 5˚ grid box using a two sided Mann-Whitney-Wilcoxon test, and a grid box is considered to be statistically significant if the p-value is less than 0.1. We note that very small portion of the changes is statistically significant for the most intense category cat 4-5 (Fig.5a). The areas of statistically significant changes increase for the less intense tropical cyclone categories (Fig. 5b-d). However, the changes are not statistically significant in many areas even for all tropical storms (cat 0-5). By comparing Fig. 4d and Fig. 5d, we note that the areas of increasing TC days of all tropical storms (cat 0-5) are not statistically significant.

According to a simple statistical significance test, only a small portion of the changes in very intense tropical cyclones (Fig. 4a) is statistically significant. However, this does not necessarily mean that the changes shown in Fig. 4a are not reliable at all. The pattern of the changes is systematic and robust among different intensity categories. It could be physically reliable even though a simple statistical significance test could not prove it.

213

214 (b) Effect of ensemble average

215 An advantage of statistical downscaling method is that it can use many data from
216 ensemble experiments. This enables us to estimate a more reliable statistics than by a
217 single experiment. Figure 6 shows the pattern of the changes in TC days of very intense
218 tropical cyclones (cat 4-5) for four individual experiments (Fig.6a-d) and ensemble
219 mean of the four experiments (Fig. 6e). The four experiments are the same model
220 simulations but only the initial conditions are different from each other. The pattern of
221 estimated TC day changes by individual model is considerably noisy (Fig.6a-d),
222 indicating that the data sample size is too small to make a reliable estimate the changes
223 at each grid box. The pattern of ensemble mean changes (Fig. 6e) is less noisy and
224 resemble to the all member ensemble mean pattern shown in Fig. 4a, indicating that the
225 four member ensemble mean estimate is more reliable than the individual model
226 estimates.

227 Figure 7 shows the pattern of the changes estimated by the other four experiments
228 (Fig. 7 a-d) and their ensemble mean (Fig. 7e). The four models are different from each
229 other by resolution (20km or 60km) and convection scheme (AS or YS). There are
230 considerable differences among the changes estimated by individual experiments. Only
231 the experiment with 60km resolution and YS convection scheme (Fig. 7b) shows a
232 decreasing TC day pattern over the Northeast Pacific and North Atlantic, but it is
233 difficult to say that this is due to resolution or convection scheme or both. Comparing
234 Fig. 7a (Fig. 7c) and Fig.7b (Fig. 7d) indicates that YS convection scheme tend to show
235 more decreasing TC day trend over the Northeast Pacific and North Atlantic. Similarly,
236 comparing Fig. 7a (Fig. 7b) and Fig. 7c (Fig. 7d), lower resolution (60km grid) models
237 tend to show more decreasing TC day trend over these ocean basins.

238

239 (c) Intensity bias correction

240 The method of statistical downscaling in the present study is based on an intensity
241 bias correction. We applied the statistical bias correction for each 5 degree latitude band
242 in the each ocean basin. An advantage of this method is that we can make bias

corrections depending on the latitudes. It should be noted that this method cannot make bias correction depending on longitudes. A slow developing bias in a simulated westward moving tropical cyclone is likely to cause a westward intensity bias (more intense in the western part of the track). We note that over the South China Sea the simulated frequency of very intense tropical cyclones (Fig. 3b) is much larger than that of observation (Fig. 3a). This is probably due to the westward intensity bias, indicating that this bias is not corrected by our bias correction method.

An obvious limitation of the statistical bias correction method of the present study is that the statistical sample size is not sufficient at high latitudes or for very intense tropical cyclones. To make a more reliable bias correction, much larger number of ensemble experiments may be necessary.

5. Conclusions

We have presented a projection of changes in the frequency of intense tropical cyclones in the future warmer climate estimated by a statistical downscaling of ensemble of many high-resolution global model experiments. The experiments include 11 member 25 year present day (PD) climate simulations and 29 member 25 year future global warming (GW) climate simulations, using MRI-AGCM 3.1 or 3.2, with different initial conditions, different convection schemes (AS, KF or YS), different resolution (20km or 60km) and different SST changes for GW climate simulations. The results indicate that the changes in the frequency (TC days) of the very intense tropical cyclones (category 4-5, Vmax≥59m/s) are not uniform on the globe. The frequency will increase in most regions but decrease in the south western part of Northwestern Pacific, the South Pacific, and eastern part of the South Indian Ocean. It is interesting to note that the pattern of the changes in TC days shown in Fig. 3d is similar to that shown in Knutson et al. (2015). The pattern of changes in the frequency of major hurricanes (category 3-5, Vmax≥50m/s) is similar to that of very intense tropical cyclones, with a little larger area of decreasing frequency. The patterns of changes in the frequency of

less intense tropical cyclones (category 1-5, Vmax ≥33m/s or cat 0-5, Vmax ≥17m/s) are also similar to that of the intense tropical cyclones, but the area of decreasing frequency systematically expands for less intense tropical cyclones, and in cat 0-5 the areas of decreasing TC days dominate the entire globe.

According to a simple statistical significance test, only a small portion of the changes in very intense tropical cyclones is statistically significant (Fig. 5). However, the pattern of the changes is systematic and robust among different intensity categories (Fig.6). It could be physically reliable even though a simple statistical significance test could not prove it. To make a more reliable, more statistically significant and more quantitative projection of the occurrence frequency of intense tropical cyclones, we need larger number of ensemble experiments, as well as an improvement in the method of statistical downscaling. These are important subjects of future work.

Acknowledgements

This work was conducted under the framework of the Program for Risk Information on Climate Change (SOUSEI program) and Innovative Program of Climate Change Projection for the 21st Century (KAKUSHIN Program) of the Ministry of Education, Culture, Sports, Science and Technology (MEXT) of Japan. Calculations were performed on the Earth Simulator of JAMSTEC.

References

Arakawa A, Schubert WH (1974) Interaction of cumulus cloud ensemble with the large-scale environment. Part I. J Atmos Sci 31:674–701

IPCC (2013) Climate Change 2013: The Physical Science Basis. T. F. Stocker et al., Eds., Cambridge University Press, 1535 pp.

Kain JS, Fritsch JM (1990) A one-dimensional entraining/detraining plume model and its application in convective parameterization. J Atmos Sci 47:2784–2802

Kain JS, Fritsch JM (1993) Convective parameterization for mesoscale models: the Kain–Fritsch scheme. In: Emanuel KA, Raymond DJ (eds) The representation of cumulus convection in numerical models of the atmosphere. Meteorology Monogr Am Meteor Soc 46:165–170

Knutson TR et al (2010) Tropical cyclones and climate change. Nat. Geosci., 3:157–163, doi:10.1038/ngeo779.

Knutson TR et al (2013) Dynamical downscaling projections of twenty-first-century Atlantic hurricane activity: CMIP3 and CMIP5 model-based scenario. J Clim 26:6591–6617. doi:10.1175/JCLI-D-12-00539.1.

Knutson TR, Sirutis JJ, Zhao M, Tuleya RE, Bender MO, Vecchi GA, Villarini G, Chavas D (2015) Global projections of intense tropical cyclone activity for the late twenty-first century from dynamical downscaling of CMIP5/RCP4.5 scenarios, J Clim 28:7203-7224. doi: 10.1175/JCLI-D-15-0129.1

Murakami H, Mizuta R, Shindo E (2012a) Future changes in tropical cyclone activity

323 projected by multi-physics and multi-SST ensemble experiments using the
324 60-km-mesh MRIAGCM. Clim Dyn., 39, 2569–2584,
325 doi:10.1007/s00382-011-1223-x.
326
327 Murakami H et al (2012b) Future changes in tropical cyclone activity projected by the
328 new high-resolution MRI-AGCM. J Clim 25:3237–3260,
329 doi:10.1175/JCLI-D-11-00415.1.
330
331 Murakami H et al (2015) Simulation and prediction of category 4 and 5 hurricanes in
332 the high-resolution GFDL HiFLOR coupled climate model. J Clim 28:9058-9079.
333 doi:10.1175/JCLI-D-15-0216.s1.
334
335 Randall D, Pan D-M (1993) Implementation of the Arakawa–Schubert cumulus
336 parameterization with a prognostic closure. The representation of cumulus
337 convection in numerical models. Meteor Monogr Am Meteor Soc 46:137–144
338
339 Roberts M et al (2015) Tropical cyclones in the UPSCALE ensemble of high-resolution
340 global climate models. J Clim 28:574-596. doi:10.1175/JCLI-D-14-00131.1.s1
341
342 Sugi M, Yoshimura J (2012) Decreasing trend of tropical cyclone frequency in 228-year
343 high-resolution AGCM simulations. Geophys Res Lett 39:L19805.
344 doi:10.1029/2012GL053360
345 Unisys (2012) Unisys weather hurricane tropical data. Available online at
346 http://weather.unisys.com/hurricane/
347
348 Walsh K et al (2016) Tropical cyclones and climate change. WIRES Clim Change
349 7:65-89. doi:10.1002/wcc.371
350
351 Wehner M, Prabhat, Reed KA, Stone D, Collins WD, J. Bacmeister J (2015) Resolution
352 dependence of future tropical cyclone projections of CAM5.1 in the U. S. CLIVAR

Hurricane Working Group idealized configurations. J. Climate, 28, 3905-3924. doi:10.1175/JCLI-D-14-00311.1

Zhao M, Held IM (2010) An analysis of the effect of global warming on the intensity of Atlantic hurricanes using a GCM with statistical refinement. J Clim 23:6382–6393. doi:10.1175/2010JCLI3837.1.

Tables

Table 1 List of experiments. P1-P11 indicates present day (PD) climate simulations, and F1-F29 indicates future global warming (GW) climate simulations. Convection schemes are AS(Arakawa-Shubert scheme, Arakawa and Schubert 1974; Randall and Pan 1993), YS (Yoshimura scheme, Yoshimura, 2016) and KF(Kain-Fritch scheme, Kain and Fritch 1990, 1993).

Table 2 Tropical cyclone numbers and their changes in various intensity categories for global domain and by ocean basin. P and F indicate ensemble average of the present day (PD) experiments and the future GW experiments, respectively. The p-values are calculated using two-sided Mann-Whitney-Wilcoxon test. Bold letters indicate that the changes are statistically significant at 90% significance level (p-value is less than 0.1).

Table 3 Same as Table 2 but for occurrence frequency (TC days) in various intensity categories for global domain and by ocean basin.

Figures

Fig. 1 Intensity bias correction based on cumulative distribution function (CDF). This figure illustrates the bias correction for the PD simulation (P7 experiment). Red, blue and green curves indicate the simulated, adjusted and observed CDF, respectively.

Fig. 2 Tropical cyclone tracks with intensity shown by colors. (a) Observed, (b) Simulated by 60km resolution model experiment (P7), (c) Adjusted by the intensity bias correction.

Fig. 3 Occurrence frequency (TC days) of very intense tropical cyclones. (a) Observation, (b) Ensemble mean of all the adjusted PD simulations (P1-P11), (c) Ensemble mean of all the adjusted GW simulations (F1-F29), and (d) The difference between GW and PD simulations [(c) minus (b)]. Unit is number of days per decade in 5˚x5˚ grid box.

Fig. 4 Changes in occurrence frequency (TC days) of tropical cyclones in various intensity categories. (a) All tropical storms (cat 0-5), (b) Hurricane intensity storms (cat 1-5), (c) Major hurricanes (cat 3-5) and (d) Very intense tropical cyclones (cat 4-5).

Fig. 5 Same as Fig.4 but only the statistically significant areas, where p-value is less than 0.1, are shown.

Fig. 6 Changes in occurrence frequency of very intense tropical cyclones (cat 4-5) of individual members of PD and GW simulations with the same model but different initial conditions. (a) F13 minus P4, (b) F14 minus P5, (c) F15 minus P6, (d) F16 minus P7. (e) Ensemble mean of the four experiments [(a)-(d)].

Fig. 7 Same as Fig.6 but for members of PD and GW simulations with different resolution (60km or 20km) and different convection scheme (AS or YS). (a) F1 minus P1 [60km AS], (b) F16 minus P7 [60km YS], (c) F28 minus P10 [20km AS], (d) F29 minus P11 [20km YS]. (e) Ensemble mean of the four experiments [(a)-(d)].

414 Table 1 Experiments

ID	PD/GW	Experiment	AGCM version	Resolution	Convection scheme	SST/SSTA
P1	PD	HP0A	3.1	60km	AS	HadISST
P2	PD	HP0A_m01	3.1	60km	AS	HadISST
P3	PD	HP0A_m02	3.1	60km	AS	HadISST
P4	PD	HPA_m00	3.2	60km	YS	HadISST
P5	PD	HPA_m01	3.2	60km	YS	HadISST
P6	PD	HPA_m02	3.2	60km	YS	HadISST
P7	PD	HPA	3.2	60km	YS	HadISST
P8	PD	HPA_kf	3.2	60km	KF	HadISST
P9	PD	HPA_as	3.2	60km	AS	HadISST
P10	PD	SP0A	3.1	20km	AS	HadISST
P11	PD	SPA	3.2	20km	YS	HadISST
F1	GW	HF0A	3.1	60km	AS	CMIP3 ensemble mean
F2	GW	HF0A_m01	3.1	60km	AS	CMIP3 ensemble mean
F3	GW	HF0A_m02	3.1	60km	AS	CMIP3 ensemble mean
F4	GW	HF0A_csiro	3.1	60km	AS	CMIP3 CSIRO
F5	GW	HF0A_csiro_m01	3.1	60km	AS	CMIP3 CSIRO
F6	GW	HF0A_csiro_m02	3.1	60km	AS	CMIP3 CSIRO
F7	GW	HF0A_miroc	3.1	60km	AS	CMIP3 MIROC_high
F8	GW	HF0A_miroc_m01	3.1	60km	AS	CMIP3 MIROC_high
F9	GW	HF0A_miroc_m02	3.1	60km	AS	CMIP3 MIROC_high
F10	GW	HF0A_mri	3.1	60km	AS	CMIP3 MRI
F11	GW	HF0A_mri_m01	3.1	60km	AS	CMIP3 MRI
F12	GW	HF0A_mri_m02	3.1	60km	AS	CMIP3 MRI
F13	GW	HFA_m00	3.2	60km	YS	CMIP3 ensemble mean
F14	GW	HFA_m01	3.2	60km	YS	CMIP3 ensemble mean
F15	GW	HFA_m02	3.2	60km	YS	CMIP3 ensemble mean
F16	GW	HFA	3.2	60km	YS	CMIP3 ensemble mean
F17	GW	HFA_cluster1	3.2	60km	YS	CMIP3 cluster1
F18	GW	HFA_cluster2	3.2	60km	YS	CMIP3 cluster2
F19	GW	HFA_cluster3	3.2	60km	YS	CMIP3 cluster3
F20	GW	HFA_kf	3.2	60km	KF	CMIP3 ensemble mean
F21	GW	HFA_kf_cluster1	3.2	60km	KF	CMIP3 cluster1
F22	GW	HFA_kf_cluster2	3.2	60km	KF	CMIP3 cluster2
F23	GW	HFA_kf_cluster3	3.2	60km	KF	CMIP3 cluster3
F24	GW	HFA_as	3.2	60km	AS	CMIP3 ensemble mean
F25	GW	HFA_as_cluster1	3.2	60km	AS	CMIP3 cluster1
F26	GW	HFA_as_cluster2	3.2	60km	AS	CMIP3 cluster2
F27	GW	HFA_as_cluster3	3.2	60km	AS	CMIP3 cluster3
F28	GW	SF0A	3.1	20km	AS	CMIP3 ensemble mean
F29	GW	SFA	3.2	20km	YS	CMIP3 ensemble mean

415

Table 2 TC number

	Global	North Indian	Northwest Pacific	Northeast Pacific	North Atlantic	South Indian	South Pacific
TC number cat 0-5							
OBS	84.8	4.8	26.5	17.1	10.4	16.3	9.8
P	84.0	6.1	22.7	19.2	6.2	18.3	11.6
F	66.6	5.5	17.6	14.7	5.0	15.5	8.4
F-P	**-17.4**	-0.6	**-5.1**	-4.5	**-1.2**	**-2.8**	**-3.3**
(F-P)/P (%)	**-20.7**	-10.1	**-22.5**	-23.5	**-19.2**	**-15.0**	**-27.9**
p-value	**0.00**	0.21	**0.04**	0.19	**0.02**	**0.00**	**0.00**
TC number cat 1-5							
OBS	47.8	1.6	17.0	9.7	5.8	8.6	5.1
P	55.6	3.0	15.6	15.5	4.3	10.7	6.6
F	48.4	3.1	13.5	12.2	3.8	10.7	5.2
F-P	**-7.2**	0.1	-2.1	-3.3	-0.5	0.0	**-1.4**
(F-P)/P (%)	**-12.9**	4.4	-13.3	-21.5	-12.4	0.4	**-21.5**
p-value	**0.06**	0.61	0.17	0.32	0.12	0.98	**0.02**
TC number cat 3-5							
OBS	22.8	0.6	8.8	4.8	2.1	4.2	2.2
P	26.0	1.1	8.0	7.6	2.0	4.8	2.5
F	24.5	1.4	7.6	6.5	2.0	5.0	2.0
F-P	-1.5	0.2	-0.4	-1.2	0.1	0.2	**-0.5**
(F-P)/P (%)	-5.8	21.1	-4.6	-15.2	3.6	3.9	**-18.9**
p-value	0.84	1.00	0.33	0.87	0.75	0.68	**0.08**
TC number cat 4-5							
OBS	14.4	0.4	6.2	3.2	1.2	2.4	1.0
P	12.1	0.5	4.9	2.3	1.1	2.2	1.0
F	12.0	0.6	4.7	2.2	1.3	2.4	0.8
F-P	-0.1	0.1	-0.2	-0.1	0.1	0.2	-0.2
(F-P)/P (%)	-0.7	21.2	-3.9	-4.4	12.4	8.2	-20.2
p-value	0.87	0.82	0.64	0.63	0.86	0.70	0.11

Table 3 TC days

	Global	North Indian	Northwest Pacific	Northeast Pacific	North Atanticl	South Indian	South Pacific
tcdays cat 0-5							
OBS	419.5	13.8	149.8	76.5	52.5	80.9	46.2
P	361.3	19.4	103.9	74.2	27.5	87.2	49.1
F	281.3	17.9	76.2	57.7	22.0	74.7	32.8
F-P	**-80.0**	-1.6	**-27.7**	-16.5	**-5.5**	**-12.5**	**-16.3**
(F-P)/P(%)	**-22.1**	-8.0	**-26.7**	-22.2	**-19.9**	**-14.3**	**-33.2**
p-value	**0.00**	0.33	**0.02**	0.22	**0.06**	**0.02**	**0.00**
tcdays cat 1-5							
OBS	173.6	2.9	71.3	32.2	23.0	29.0	15.2
P	175.8	5.6	56.0	43.6	14.3	36.2	20.1
F	157.0	6.9	47.9	36.0	13.1	38.7	14.5
F-P	-18.8	1.3	-8.2	-7.7	-1.1	2.5	**-5.5**
(F-P)/P(%)	-10.7	22.6	-14.6	-17.6	-8.0	6.8	**-27.5**
p-value	0.09	0.91	0.11	0.41	0.25	0.73	**0.01**
tcdays cat 3-5							
OBS	51.1	0.8	23.7	9.3	5.1	8.2	3.8
P	59.7	1.8	21.2	15.2	4.8	11.2	5.6
F	61.2	2.6	21.4	13.9	5.3	13.8	4.3
F-P	1.5	0.8	0.1	-1.4	0.5	2.6	**-1.3**
(F-P)/P(%)	2.5	48.0	0.7	-8.9	10.7	23.3	**-22.5**
p-value	0.87	0.52	0.54	0.86	0.70	0.16	**0.02**
tcdays cat 4-5							
OBS	26.6	0.4	14.2	4.1	2.6	3.8	1.6
P	21.8	0.5	10.3	3.4	2.1	3.5	1.9
F	25.0	0.9	11.5	3.6	2.6	4.9	1.6
F-P	3.3	0.4	1.1	0.2	0.5	**1.4**	-0.3
(F-P)/P(%)	15.0	68.5	10.9	6.2	21.3	**39.1**	-15.7
p-value	0.30	0.48	0.79	0.82	0.66	**0.04**	0.13

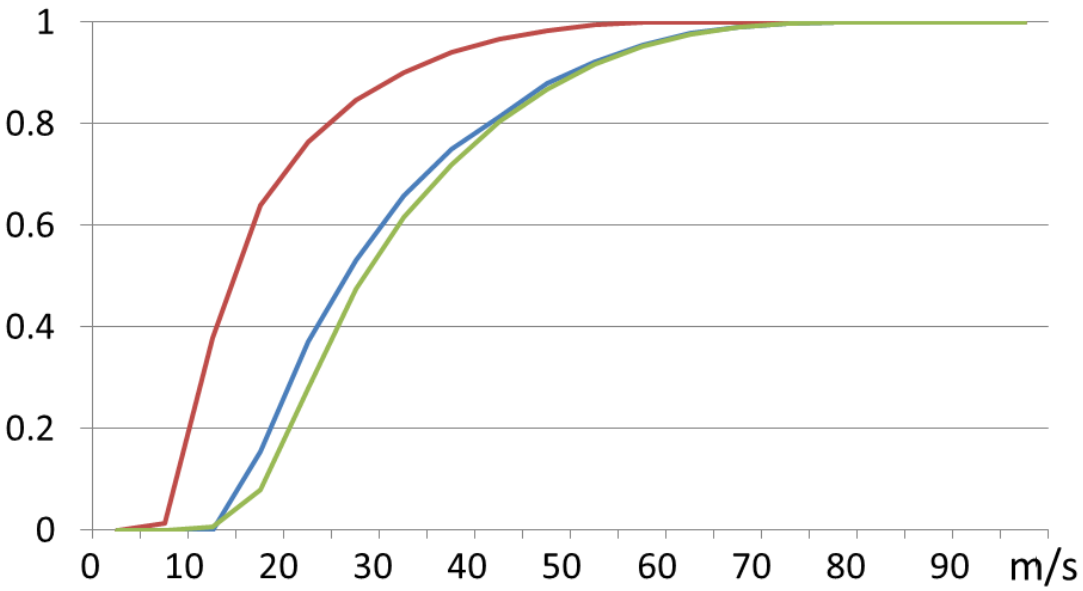

Fig. 1 Intensity bias correction based on cumulative distribution function (CDF). This figure illustrates the bias correction for the PD simulation (P7 experiment). Red, blue and green curves indicate the simulated, adjusted and observed CDF, respectively.

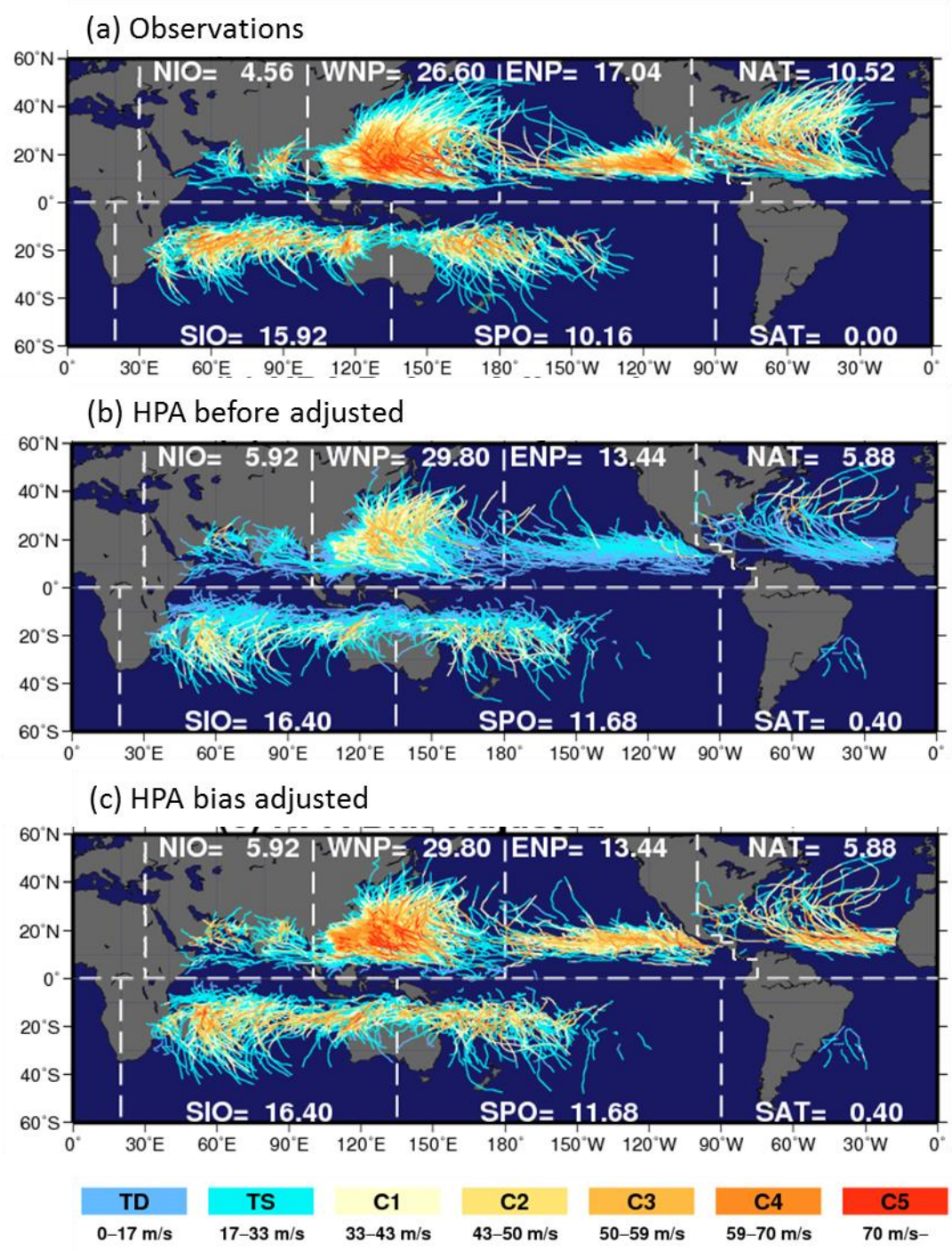

Fig. 2 Tropical cyclone tracks with intensity shown by colors. (a) Observed, (b) Simulated by 60km resolution model experiment (P7), (c) Adjusted by the intensity bias correction.

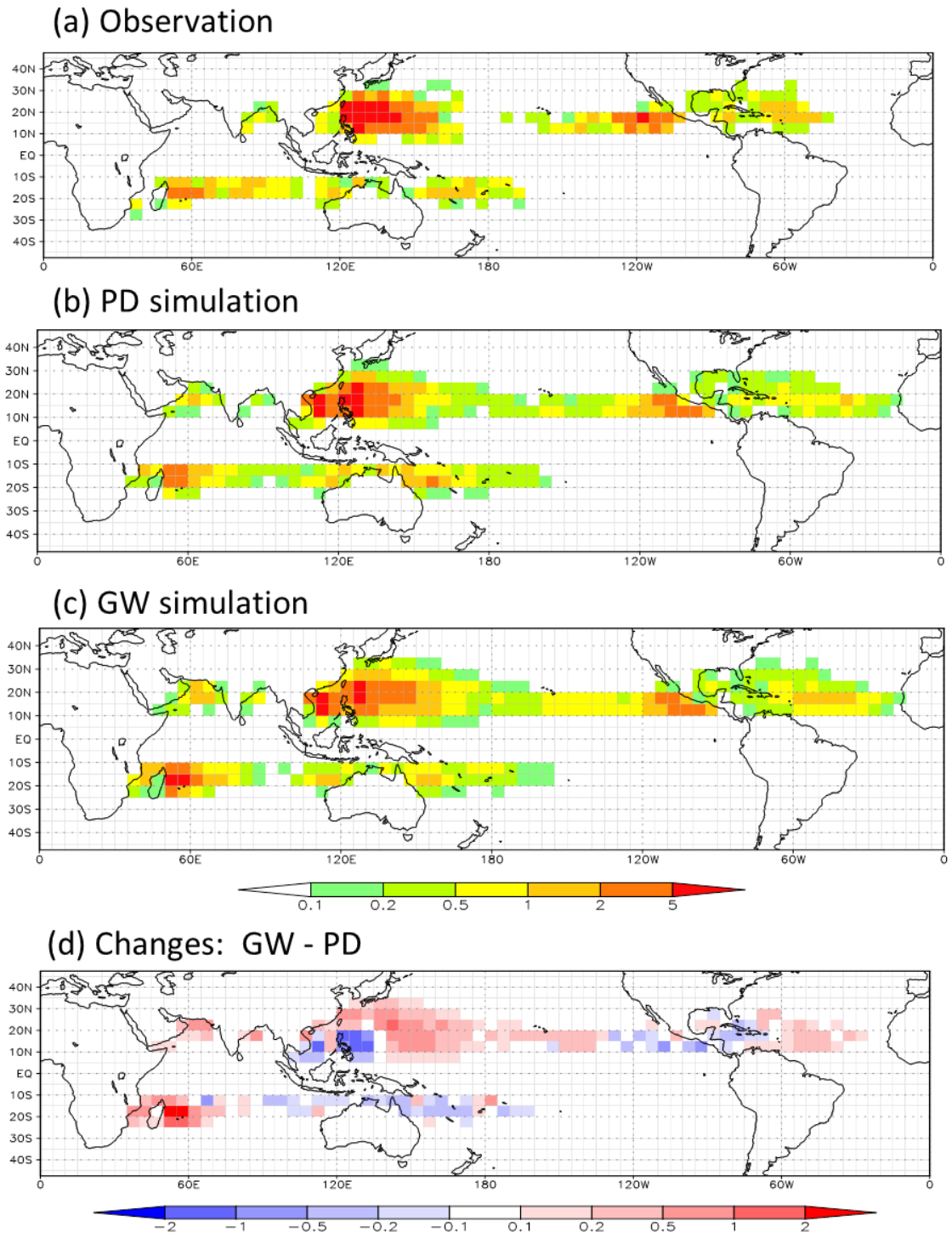

Fig. 3 Occurrence frequency (TC days) of very intense tropical cyclones. (a) Observation, (b) Ensemble mean of all the adjusted PD simulations (P1-P11), (c) Ensemble mean of all the adjusted GW simulations (F1-F29), and (d) The difference between GW and PD simulations [(c) minus (b)]. Unit is number of days per decade in 5˚x5˚ grid box.

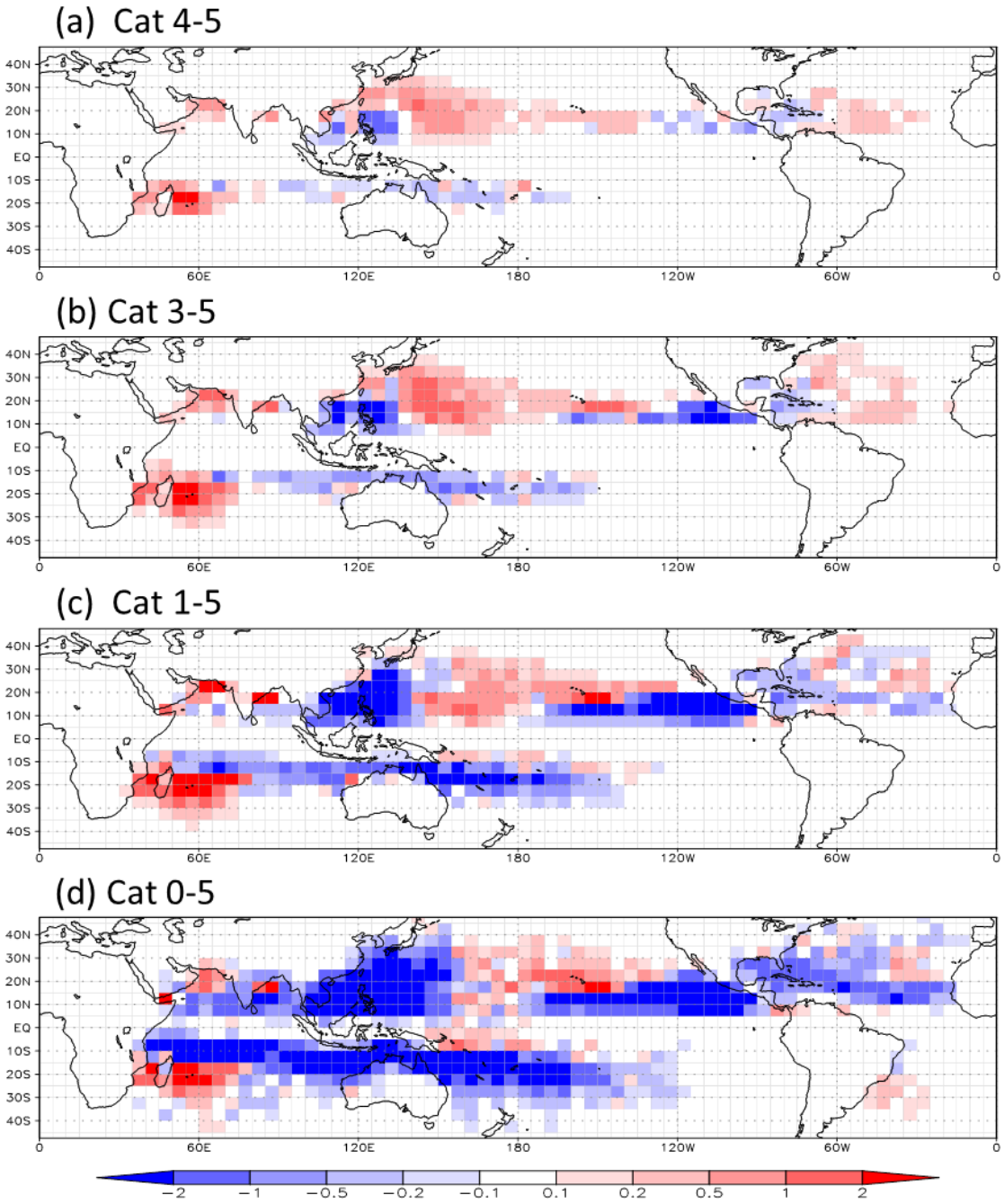

Fig. 4 Changes in occurrence frequency (TC days) of tropical cyclones in various intensity categories. (a) All tropical storms (cat 0-5), (b) Hurricane intensity storms (cat 1-5), (c) Major hurricanes (cat 3-5) and (d) Very intense tropical cyclones (cat 4-5).

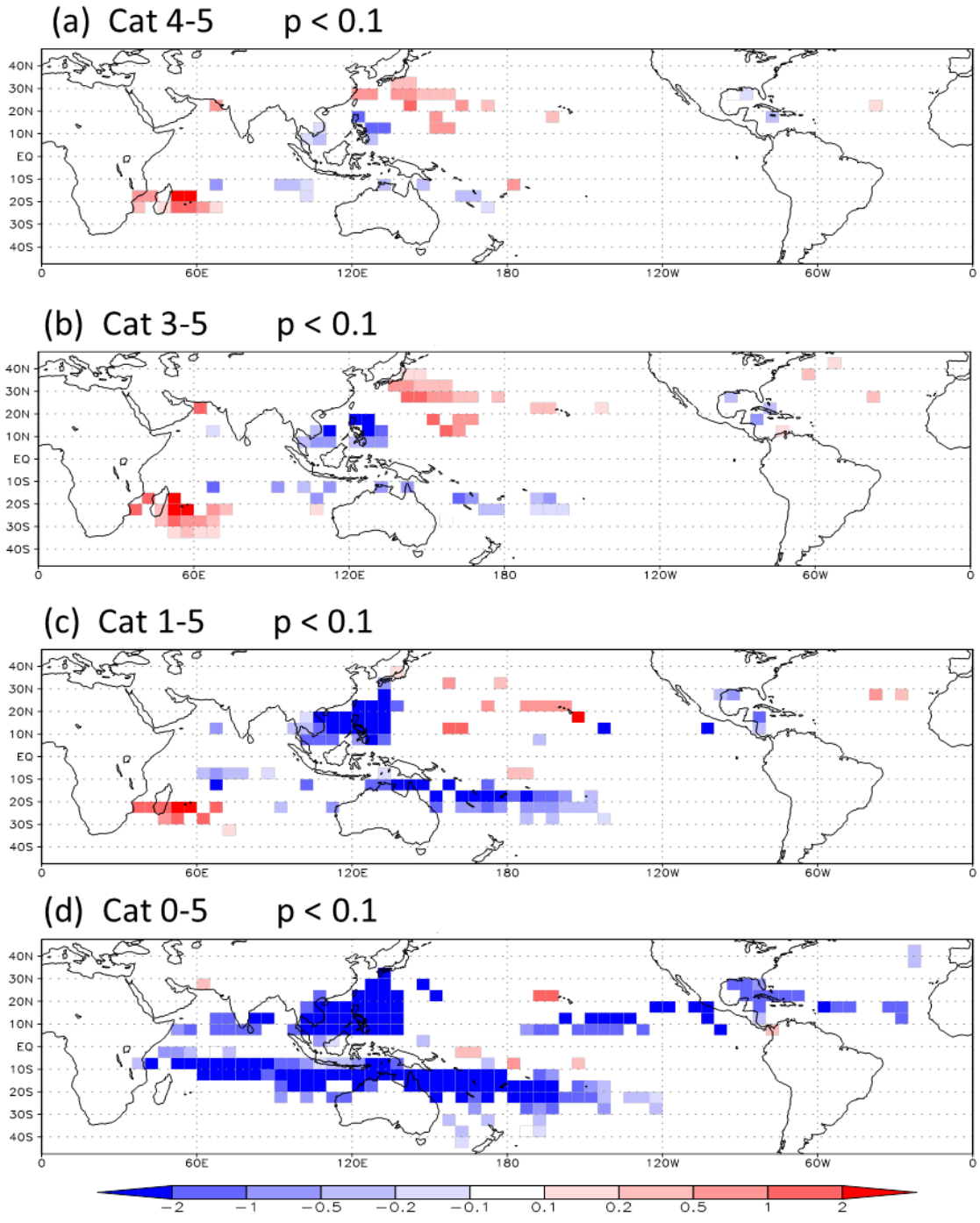

Fig. 5 Same as Fig.4 but only the statistically significant areas, where p-value is less than 0.1, are shown.

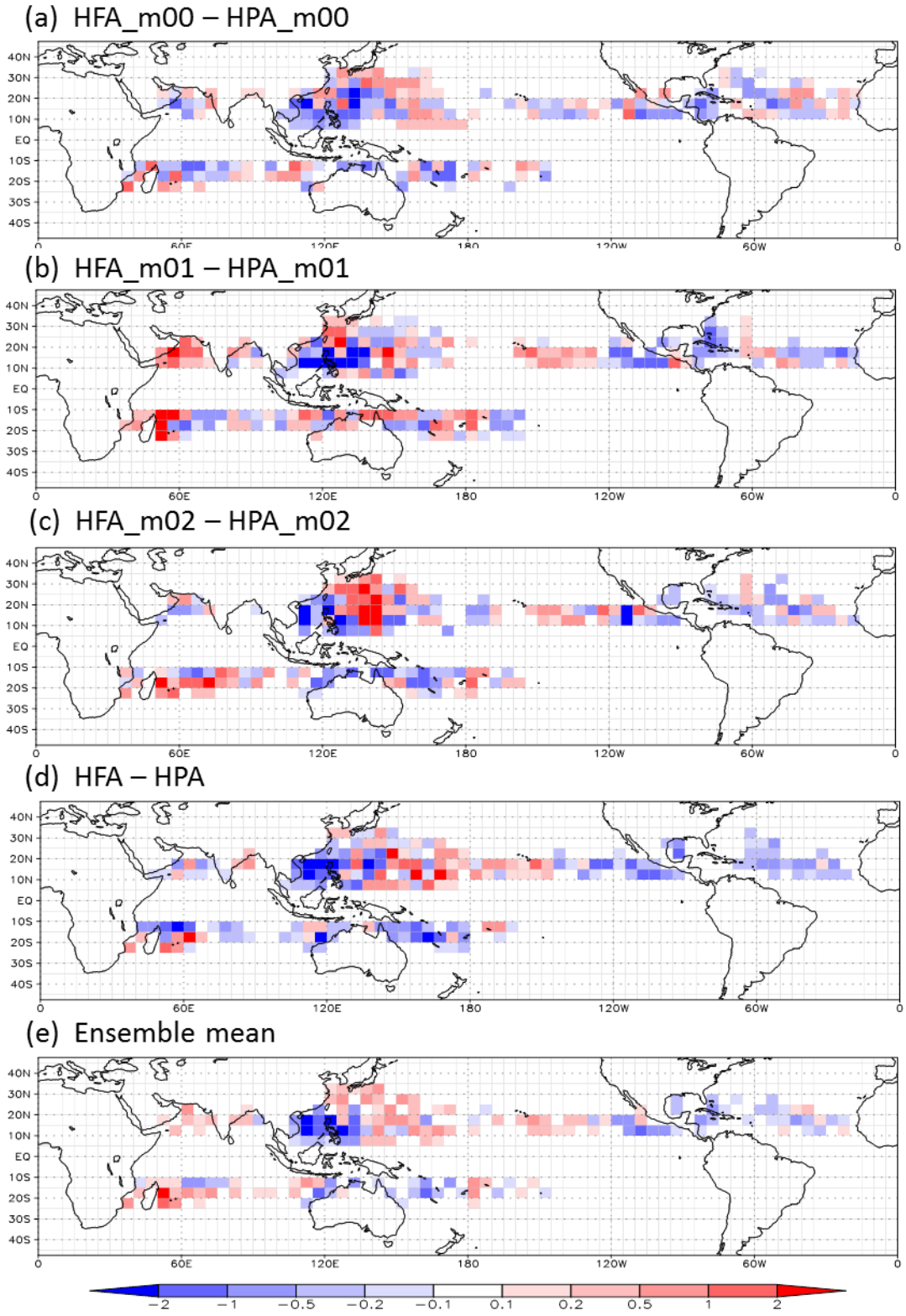

Fig. 6 Changes in occurrence frequency of very intense tropical cyclones (cat 4-5) of individual members of PD and GW simulations with the same model but different initial conditions. (a) F13 minus P4, (b) F14 minus P5, (c) F15 minus P6, (d) F16 minus P7. (e) Ensemble mean of the four experiments [(a)-(d)].

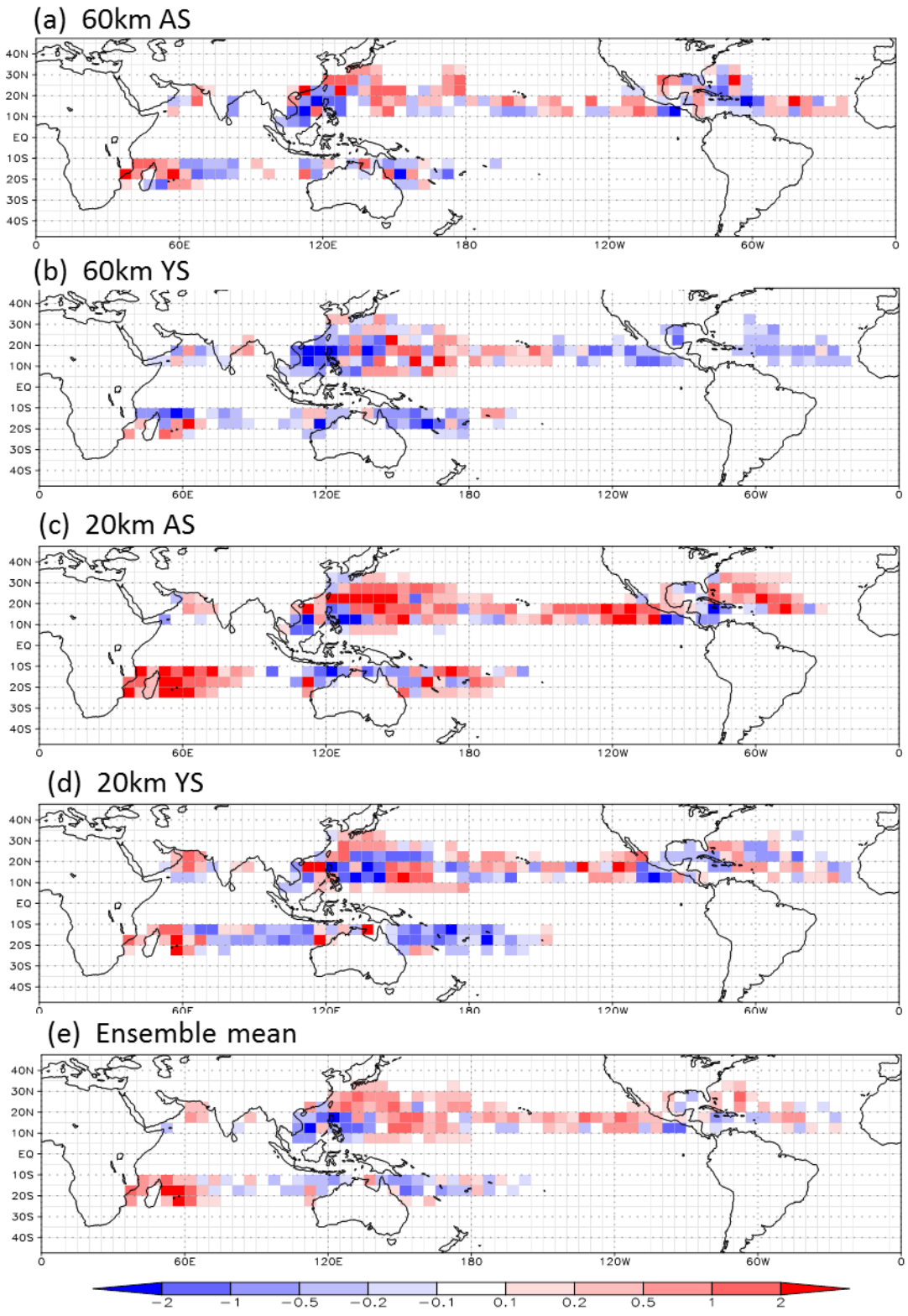

Fig. 7 Same as Fig.6 but for members of PD and GW simulations with different resolution (60km or 20km) and different convection scheme (AS or YS). (a) F1 minus P1 [60km AS], (b) F16 minus P7 [60km YS], (c) F28 minus P10 [20km AS], (d) F29 minus P11 [20km YS]. (e) Ensemble mean of the four experiments [(a)-(d)].